Cell

A *trans*-Acting Riboswitch Controls Expression of the Virulence Regulator PrfA in *Listeria monocytogenes*

Edmund Loh,[1,2,7] Olivier Dussurget,[3,4,5,7] Jonas Gripenland,[1,2,7] Karolis Vaitkevicius,[1,2] Teresa Tiensuu,[1,2] Pierre Mandin,[3,4,5,8] Francis Repoila,[3,4,5,9] Carmen Buchrieser,[6] Pascale Cossart,[3,4,5,*] and Jörgen Johansson[1,2,*]
[1]Department of Molecular Biology
[2]Laboratory for Molecular Infection Medicine Sweden
Umeå University, 90187 Umeå, Sweden
[3]Institut Pasteur, Unité des Interactions Bactéries-Cellules, Paris F-75015, France
[4]INSERM U604, Paris F-75015, France
[5]INRA USC2020, Paris F-75015, France
[6]Institut Pasteur, UP Biologie des Bactéries Intracellulaires, CNRS URA 2171, Paris F-75724, France
[7]These authors contributed equally to this work
[8]Present address: Laboratory of Molecular Biology, Center for Cancer Research, National Cancer Institute, Bethesda, MD 20892, USA
[9]Present address: INRA UR888, Jouy-en-Josas F-78352, France
*Correspondence: pcossart@pasteur.fr (P.C.), jorgen.johansson@molbiol.umu.se (J.J.)
DOI 10.1016/j.cell.2009.08.046

SUMMARY

Riboswitches are RNA elements acting in *cis*, controlling expression of their downstream genes through a metabolite-induced alteration of their secondary structure. Here, we demonstrate that two *S*-adenosylmethionine (SAM) riboswitches, SreA and SreB, can also function in *trans* and act as noncoding RNAs in *Listeria monocytogenes*. SreA and SreB control expression of the virulence regulator PrfA by binding to the 5′-untranslated region of its mRNA. Absence of the SAM riboswitches SreA and SreB increases the level of PrfA and virulence gene expression in *L. monocytogenes*. Thus, the impact of the SAM riboswitches on PrfA expression highlights a link between bacterial virulence and nutrient availability. Together, our results uncover an unexpected role for riboswitches and a distinct class of regulatory noncoding RNAs in bacteria.

INTRODUCTION

Noncoding RNAs (ncRNAs) have been assigned a variety of functions in both eubacteria and eukaryotes, where they generally act on distally encoded target mRNAs. In bacteria, ncRNAs control multiple biological processes, including virulence (Johansson and Cossart, 2003; Romby et al., 2006; Toledo-Arana et al., 2007). They act either by sequestering target proteins or by an antisense mechanism through base-pairing, usually in the region of the ribosomal binding site of the target mRNA (Guillier et al., 2006; Vogel and Wagner, 2007). Binding of the ncRNA to the 5′ untranslated region (5′ UTR) region of the mRNA often inhibits translation, and the corresponding transcript is in most cases degraded. In recent years, ncRNAs have been identified and characterized in many different pathogenic bacteria (Toledo-Arana et al., 2007). For instance, RNAIII of *Staphylococcus aureus* has been shown to directly control the fate of several mRNA targets involved in virulence by RNA:RNA interactions (Boisset et al., 2007). In *Listeria monocytogenes*, more than 40 ncRNAs have been identified, with at least two being involved in virulence (Toledo-Arana et al., 2009).

Expression of the virulence regulator PrfA of *L. monocytogenes* was previously shown to be controlled by a thermosensor located at the 5′ UTR of the *prfA* transcript (Johansson et al., 2002). At low temperatures (<30°C), the 5′ UTR of *prfA* forms a secondary structure that masks the Shine-Dalgarno (SD) site and prevents translation. At higher temperatures (37°C), this secondary hairpin structure is partially disrupted, enabling binding of the ribosome and translation initiation.

It was recently discovered that certain 5′ UTRs, termed riboswitches, could control expression of their downstream genes by directly binding a ligand, often being the end products in the metabolic pathway encoded by the downstream genes (Nudler, 2006; Lu et al., 2008; Roth and Breaker, 2009). For example, by binding their effector molecule *S*-adenosylmethionine (SAM), some SAM riboswitches form a termination structure that terminates transcription and inhibits synthesis of the downstream mRNA (see Figure S1 available online) (McDaniel et al., 2003; Winkler et al., 2003; Whitford et al., 2009). In the absence of SAM, an antiterminator structure is instead formed and transcription proceeds. We have tested whether terminated SAM riboswitches could function as ncRNAs and control the expression of *trans*-encoded target mRNAs via a direct interaction. We report here that two SAM riboswitches in *L. monocytogenes* act as ncRNAs by interacting with the 5′ UTR of the mRNA encoding the master regulator of virulence, PrfA.

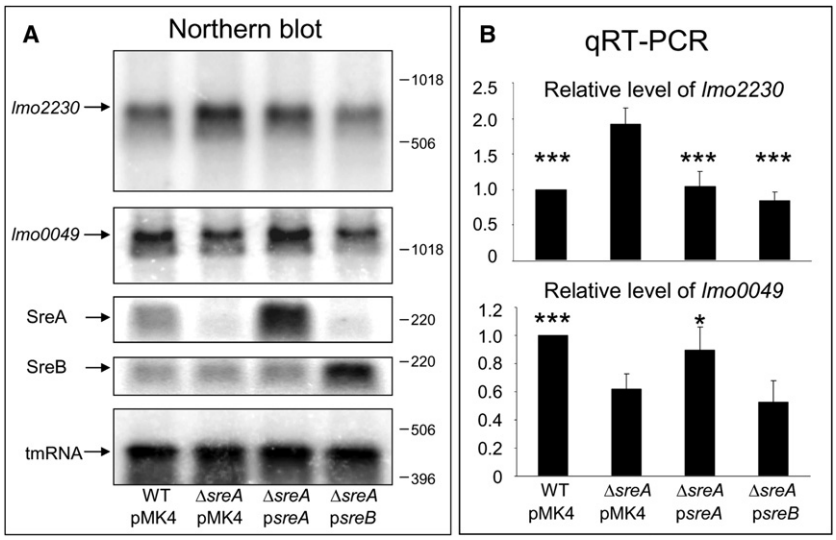

Figure 1. SAM Riboswitch Elements Can Function in *trans*

Total RNA was isolated from the indicated strains grown in BHI medium to a cell density of OD_{600} = 0.4. (A) Northern blots (n = 3) were hybridized with *lmo2230*-, *lmo0049*-, SreA-, SreB-, or tmRNA-specific DNA probes. Specific products are indicated by arrows. Sizes (bases) are indicated to the right of the northern blots.

(B) Quantitative real-time-PCR (qRT-PCR) analysis was performed using *lmo2230*-, *lmo0049*-, and tmRNA-specific primers. Bars indicate the relative expression of *lmo2230* and *lmo0049* in relation to tmRNA (control) shown as mean values with standard deviations (n = 5, except for Δ*sreA*+p*sreB*, where *lmo2230* and *lmo0049* measurements was repeated 4 and 2 times, respectively). All samples were compared to Δ*sreA* + pMK4 using Student t test (two-tailed) (*** $p < 0.001$; * $p < 0.05$).

Absence of a SAM Riboswitch Alters Expression of *trans*-Encoded mRNAs

L. monocytogenes harbors seven putative SAM riboswitches (also denoted as S-box or SAM-I) (Henkin, 2008; Roth and Breaker, 2009) that were identified by tiling arrays and were named Sre (*S*AM *r*iboswitch *e*lement) (Toledo-Arana et al., 2009) (Table S1). These potential riboswitch elements, designated SreA-G, are situated upstream of genes encoding proteins involved in methionine and cysteine transport/metabolism and have conserved regions (Figures S2 and S3). Several lines of evidence indicate that these RNA elements constitute canonical riboswitches that terminate transcription upon binding SAM: (1) The core sequence regions of the seven RNA species show a high degree of identity to SAM riboswitches acting at the transcription level (Figure S3) (Winkler et al., 2003; Griffiths-Jones et al., 2005). (2) One tested SAM riboswitch, SreA, was transcribed together with its downstream genes (*lmo2419-lmo2418-lmo2417*, encoding an ABC-transporter complex) at stationary phase (low-nutrient conditions, Figure S4). At logarithmic growth phase (rich condition), SreA was expressed as a short terminated transcript (229 bases, Figure S4). (3) Addition of SAM to an in vitro transcription assay caused an increased level of termination in a degree similar to what was discovered for other characterized SAM riboswitches (Figure S5) (Winkler et al., 2003). On the basis of these observations, we consider SreA-G to be canonical SAM riboswitches.

Because of their abundance and length, can terminated riboswitches function in *trans*, regulating distally located target mRNAs/proteins? To study a possible *trans*-regulatory role of riboswitch elements, we constructed a *L. monocytogenes* wild-type strain (EGDe) lacking the longest and most expressed riboswitch (SreA) (Table S1; Figures S1 and S6). The *sreA* deletion mutant still carried the native promoter to ensure expression of the downstream gene, *lmo2419* (Figure S1). The mutant displayed the same growth rate as the wild-type strain and was able to grow in minimal media (data not shown). To identify genes putatively regulated by SAM riboswitch elements, we conducted a transcriptome analysis experiment by comparing gene expression of the Δ*sreA* strain and the wild-type strain. RNA from the two strains, grown in rich conditions (brain heart infusion [BHI]) when the termination product is synthesized, was isolated from mid-logarithmic growth phase and subjected to whole genome gene-array analysis (Table S2). Three genes showed significant up-regulation, whereas six showed significant down-regulation in the Δ*sreA* strain, compared to the wild-type strain. Of these genes, two were chosen for further studies. One, *lmo2230*, encodes a protein homologous to bacterial arsenate reductase and showed increased expression in the Δ*sreA* strain. The other, *lmo0049*, encodes AgrD, which is the listerial homolog of *S. aureus* autoinducing peptide (Riedel et al., 2009). AgrD is important for biofilm formation and virulence in *L. monocytogenes* and showed reduced expression in the Δ*sreA* strain.

SreA Is Able to Function in *trans* Independently of SAM Binding

In order to test the possible *trans*-regulatory function of SreA and exclude effects caused by the downstream gene *lmo2419*, we examined the effect of complementation on expression of *trans*-regulated mRNAs. The Δ*sreA* strain was transformed with p$sreA_{wt}$ (i.e., the medium-copy number, replicative plasmid pMK4 carrying the DNA fragment encoding the SreA riboswitch [229 nucleotides], but not the downstream gene *lmo2419*; Figure S1). In this construct, SreA is under the control of its native promoter. The wild-type strain harboring pMK4, the Δ*sreA* strain carrying pMK4, and the Δ*sreA* strain carrying p$sreA_{wt}$ were grown in BHI medium to mid-logarithmic growth phase (OD_{600} = 0.4). When expressed with its native promoter in a Δ*sreA* background, SreA could significantly restore expression of *lmo2230* and *lmo0049* to a level similar to that detected in the wild-type strain, as shown by northern blotting and by quantitative reverse transcriptase-PCR (qRT-PCR) analysis (Figure 1). On the basis of their sequence homology, it could be hypothesized that other SAM riboswitches also could control expression of *lmo2230* and *lmo0049*. To test this, we inserted another SAM riboswitch, SreB, into pMK4 carrying its native promoter and

expressed in the Δ*sreA* strain. Expression of *lmo2230* in that strain was significantly restored to the level observed in the wild-type strain carrying pMK4 and the Δ*sreA* strain carrying p*sreA*$_{wt}$ (Figure 1). In contrast, SreB was not able to restore expression of *lmo0049* to the levels observed in the Δ*sreA* strain harboring p*sreA*$_{wt}$. This suggests that the *trans*-regulatory effect of SreA on *lmo2230* and *lmo0049* expression is exerted by two different mechanisms.

In order to investigate whether the binding of SAM to the riboswitch element is essential for the *trans*-effect observed, we constructed a riboswitch element unable to bind SAM and to form an antitermination structure (Figure 2A). For such a construct, two residues conserved in 1179 of 1182 known/predicted SAM riboswitch elements in different species were altered in the core of the metabolite-binding domain (GA→AG at position 61–62; Figure S3) (Winkler et al., 2003; Griffiths-Jones, et al., 2005; Montange and Batey, 2006). Identical base substitutions in a corresponding riboswitch element in *Bacillus subtilis* have previously been shown to prevent SAM binding (Winkler et al., 2003). To obtain the short transcript in the absence of SAM binding, we also introduced base-substitution mutations disrupting the formation of an antitermination structure in the construct. The final construct was named p*sreA*$_{NSB}$ (*n*on-SAM-*b*inding SreA). As predicted, a short transcript with a size identical to SreA was produced at logarithmic growth phase (Figure 2A, right inset). In the Δ*sreA* strain harboring p*sreA*$_{NSB}$, the expression of *lmo2230* was significantly restored to the level observed in the wild-type strain supplemented with pMK4 or Δ*sreA* supplemented with p*sreA*$_{wt}$, showing that SreA control *prfA* expression independently of SAM binding (Figure 2B).

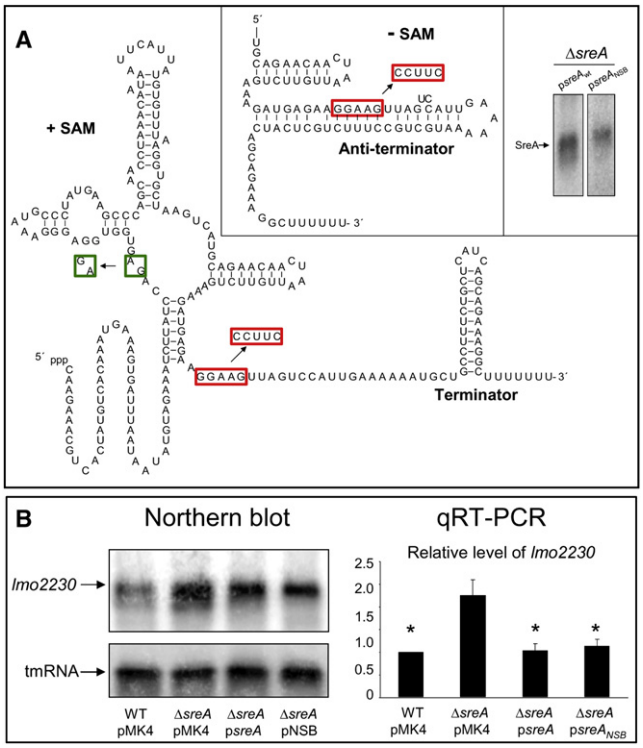

Figure 2. The *trans* Function of SreA Is Independent of SAM Binding

(A) Sequence and structural model of the SreA riboswitch in two structural states. Sequences boxed in green indicate base-substitution mutations introduced to eliminate SAM binding (Winkler et al., 2003). Sequences boxed in red indicate base-substitution mutations introduced to prevent formation of an antitermination structure. Structure model of wild-type SreA in the presence of SAM (large picture) or in the absence of SAM (left inset). Northern blot analysis of SreA expression in the Δ*sreA* + p*sreA*$_{wt}$ and the Δ*sreA* + p*sreA*$_{NSB}$ strains grown to OD_{600} = 0.4 (right inset). Membrane was hybridized with SreA-specific ^{32}P-labeled PCR amplified fragments. The SreA transcript is shown by an arrow.

(B) Analysis of *lmo2230* and tmRNA expression. Total RNA was isolated from indicated strains grown in BHI medium to a cell density of OD_{600} = 0.4. Northern blots (n = 3) were hybridized with *lmo2230* or tmRNA-specific ^{32}P-labeled PCR amplified fragments. Specific products are indicated by arrows. For qRT-PCR analysis (n = 3), either 5 ng (*lmo2230*) or 250 pg (tmRNA) of each RNA sample was used with *lmo2230* and tmRNA specific primers. Bars indicate the relative expression of *lmo2230* in relation to tmRNA (control) as the means with standard deviations. All samples were compared to Δ*sreA* + pMK4 using Student t test (two-tailed) and showed a significant difference against Δ*sreA*+pMK4 (* $p < 0.05$).

SreA Controls Expression of the Virulence Regulator PrfA

Expression of *lmo2230* has been shown to be activated by two regulators, the sigma factor σ^B and the virulence regulator PrfA (Milohanic et al., 2003). To investigate whether the increased expression of *lmo2230* in the Δ*sreA* strain was due to an altered expression of these regulators, we isolated cytoplasmic protein fractions and assessed expression of σ^B and PrfA by western blotting. The levels of σ^B, as well as the expression of a known σ^B-regulated gene (*lmo0880*), were similar in all strain backgrounds (Figure S7; data not shown). In contrast, expression of the PrfA protein increased approximately 2-fold in the strain lacking SreA, compared to the wild-type strain (Figure 3A). In the Δ*sreA* strain complemented with p*sreA*$_{wt}$, PrfA expression was reduced to a level similar to or lower than that in the wild-type strain. A similar effect of SreA on *prfA* expression could be detected at the RNA level, although the *prfA*-transcript was not reduced below wild-type levels in the Δ*sreA* supplemented with p*sreA*$_{wt}$ (Figure 3B). One of the virulence factors being controlled by PrfA is *hly*, encoding Listeriolysin O, which is essential for the bacterial escape from the phagosome. We therefore tested whether a strain lacking SreA showed an altered *hly* expression. The Δ*sreA* strain showed an increased amount of *hly*, compared with the wild-type strain (Figure 3B). The amount of *hly* was restored to wild-type levels in the Δ*sreA* strain supplemented with p*sreA*$_{wt}$ (Figure 3B). To analyze whether SreA and SreB function in concert to control expression *prfA,* we constructed a Δ*sreA*, Δ*sreB* double knockout mutant. The absence of both SreA and SreB leads to a 3-fold increased expression of *prfA*, compared to the wild-type strain (Figure 3C). This indicates that both SreA and SreB act together to control expression of *prfA*.

Expression of SreA Is Controlled by PrfA

When searching for PrfA consensus binding sites in the promoter region of SreA and SreB, we identified putative PrfA binding sites upstream of SreA and SreB (Figure 4A). This prompted us to investigate whether the expression of SreA and SreB was

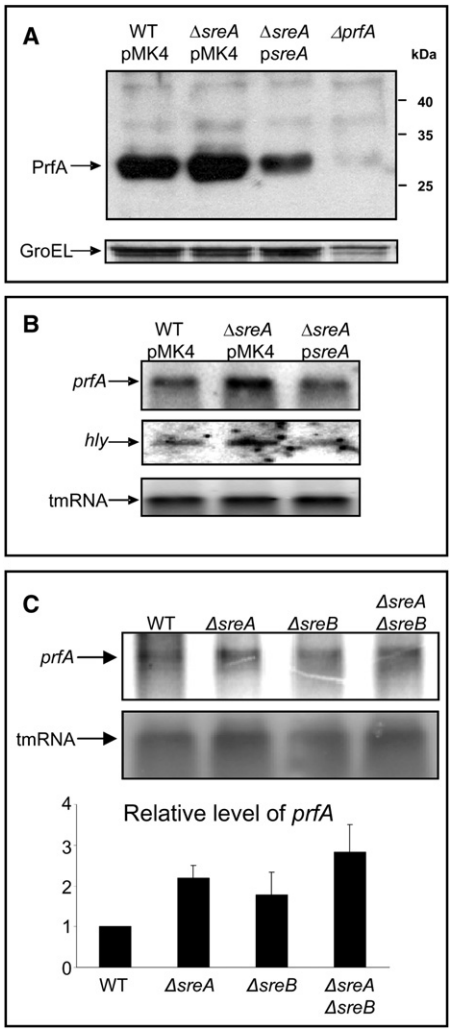

Figure 3. Expression of PrfA Is Increased in the Absence of SreA

(A) Western blot analysis of the expression levels of PrfA. Total protein was isolated from the indicated strains and was subjected to western blot analysis (n = 2). Membranes were probed with antibodies recognizing PrfA or GroEL (control).

(B) Northern blot analysis of *prfA* and *hly* expression. Total RNA was isolated from the indicated strains grown in BHI medium to a cell density of OD_{600} = 0.4 and was subjected to northern blot analysis (n = 3). Membranes were hybridized with *prfA*-, *hly*-, and tmRNA-specific DNA probes. Specific products are indicated by arrows.

(C) Northern blot analysis of *prfA* expression. Total RNA was isolated from indicated strains grown in BHI medium to cell density of OD_{600} = 0.4 and was subjected to northern blot analysis (n = 2). Membranes were hybridized with *prfA* and tmRNA probes. Specific products are indicated by arrows. Below is shown a quantification of the *prfA* bands on northern using STORM represented as mean with standard deviations. Expression of *prfA* is correlated to tmRNA.

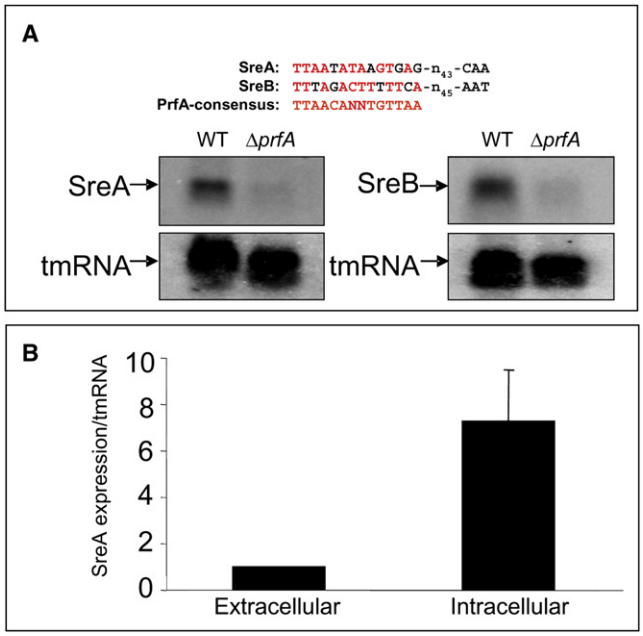

Figure 4. The SreA Riboswitch Is Controlled by PrfA and Is Induced Intracellularly

(A) Northern blot analysis of SreA expression. Total RNA was isolated from the wild-type (WT) and the Δ*prfA* strain grown in BHI medium to a cell density of OD_{600} = 1.2 and was subjected to northern blot analysis (n = 2). Membranes were hybridized with SreA-, SreB-, or tmRNA-specific DNA probes. Specific products are indicated by arrows. Suggested PrfA-binding sites lying in front of the SreA and SreB promoters are shown together with the consensus PrfA-binding site. Bases corresponding to the PrfA-binding consensus are shown in red.

(B) Intracellular expression of SreA. Wild-type *L. monocytogenes* was allowed to infect HeLa cells for 4 hr before bacteria and total RNA were isolated. As a control, *L. monocytogenes* was grown in cell-culture medium without HeLa cells before RNA was isolated (n = 3). The amount of SreA for both extracellularly and intracellularly grown bacteria was quantified using qRT-PCR, related to tmRNA and represented as mean with standard deviations.

controlled by PrfA. As demonstrated in Figure 4A, a reduction in the expression of both SreA and SreB was observed in a Δ*prfA* knockout strain. We and others have previously shown that expression of PrfA- and PrfA-regulated genes was increased after bacterial adhesion to and entry into host cells (Renzoni et al., 1999; Moors, et al., 1999; Scortti et al., 2007). It was therefore of interest to test whether SreA was induced intracellularly, thus giving support for a PrfA-mediated regulation. In agreement with this hypothesis, we found that the level of SreA was increased 7-fold after the bacteria had invaded HeLa cells (Figure 4B).

SreA and the *prfA*-UTR Interact in *Escherichia coli*

Analyzing the sequences of SreA and the 5′ UTR region of *prfA* revealed a high degree of complementarity between the paired region 3 of SreA and the distal side of the *prfA*-UTR stem (Figure 5A). When the SreA:*prfA*-UTR interaction was analyzed with the RNA_{hybrid} program (Rehmsmeier, et al., 2004), a ΔG value of −38.1 kcal/mol was calculated. To test whether SreA and *prfA* directly interact without involvement of any other listerial factor(s), we used an ectopic system in *Escherichia coli*, which does not harbor any SAM-I riboswitches or *prfA*. A plasmid expressing a *prfA-gfp* fusion (Johansson et al., 2002) was introduced into *E. coli*, together with pMK4 or $psreA_{wt}$. A similar GFP expression approach has previously been used to verify ncRNA-mRNA interactions (Urban and Vogel, 2007).

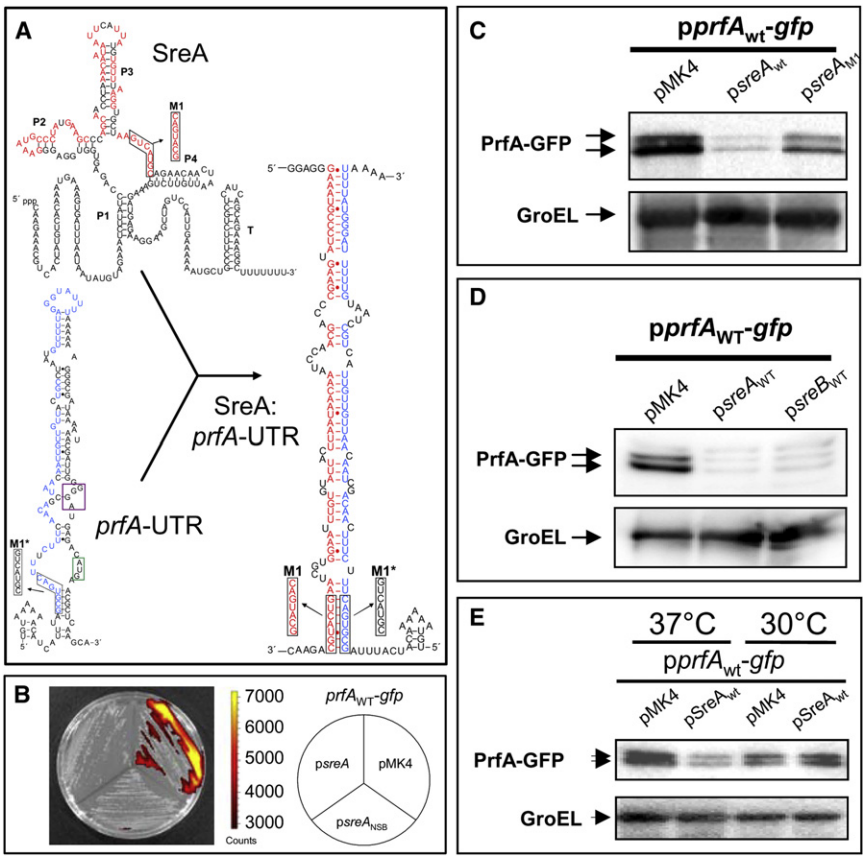

Figure 5. SreA Interacts with the *prfA*-UTR in *Escherichia coli*

(A) Predicted secondary structures of the *prfA*-UTR and SreA together with a putative interaction site as indicated by the RNA_{hybrid} program (Rehmsmeier et al., 2004). Paired regions in SreA are labeled P1 to P4 and the terminator T. The SD site and start codon of *prfA* are indicated by purple and green boxes, respectively. The suggested bases interacting between SreA and *prfA*-UTR are indicated by red letters in SreA and by blue letters in the *prfA*-UTR. Base substitution mutation constructs (M1 and M1*) are indicated in black boxes.

(B) Fluorescence measurements on agar plate. The indicated strains were streaked on LA agar-plate and grown at 37°C for 24 hr (n = 2). Fluorescence was measured with an IVIS-spectrum imaging system. Color scale represents level of fluorescence intensity ranging from high (yellow) to low (dark red).

(C) Western blotting evaluating the amount of PrfA-GFP. The indicated strains were grown to an OD_{600} of 0.4 at 37°C. Total protein was isolated from the indicated strains and subjected to western blot analysis (n = 5). Membranes were probed with antibodies recognizing GFP or GroEL (control).

(D) Expression of SreB inhibits PrfA-GFP expression. The indicated strains were grown to an OD_{600} = 0.4. Total protein was isolated and was subjected to western blot analysis (n = 3). Membranes were probed with antibodies recognizing GFP or GroEL (control).

(E) Temperature-dependent SreA repression of PrfA-GFP expression. The indicated strains were grown to an OD_{600} of 0.4 at either 30°C or 37°C. Total protein was isolated from the indicated strains and subjected to western blot analysis (n = 3). Membranes were probed with antibodies recognizing GFP or GroEL (control).

GFP expression was examined by measuring fluorescence of bacteria directly on agar plates or by western blot detection of PrfA-GFP from bacteria grown in liquid culture to an OD_{600} of 0.4. If SreA and *prfA* directly interact, the presence of SreA should decrease expression of PrfA-GFP. In line with this hypothesis, the presence of $SreA_{wt}$ dramatically reduced fluorescence of plated bacteria (Figure 5B). In addition, expressing *prfA-gfp* together with the non-SAM-binding SreA ($SreA_{NSB}$) completely repressed GFP expression in a degree similar to $SreA_{wt}$, thus further proving that the *trans*-regulatory mechanism of SreA is independent of SAM binding (Figure 5B). When bacteria were grown in liquid culture, the presence of $SreA_{wt}$ lowered the level of $PrfA_{wt}$-GFP dramatically, compared with that of the vector control (Figure 5C). The effect of SreA on *prfA* expression appears to be more pronounced in *E. coli* than in *L. monocytogenes*, possibly because no other SAM-I riboswitches are present in *E. coli*.

Mutations Weakening the Putative SreA:*prfA*-UTR Interaction Increase PrfA Expression

By analyzing the putative SreA:*prfA*-UTR interaction site, a more GC-rich region was detected at the base of the stem (Figure 5A). Several base substitutions that increased the theoretical ΔG value (from −38.1 to approximately −27 kcal/mol) were introduced into either SreA (M1) or *prfA* (M1*) (Figure 5A). If $SreA_{wt}$ and $prfA_{wt}$ directly interact, such base substitutions should weaken the repressive effect by SreA on PrfA-GFP expression. Indeed, repression by SreA was nearly abolished when $SreA_{M1}$ was expressed in the presence of $prfA_{wt}$-*gfp* as determined by analyzing protein levels from bacteria grown in liquid culture (Figure 5C).

Making the reciprocal experiment was not possible: Base substitutions in the *prfA*-UTR (M1*) that destabilize a putative SreA:*prfA* interaction also disrupt base pairing in the bottom part of the *prfA*-thermosensor (Figure 5A) (Johansson et al., 2002). Because the SD region of the *prfA*-thermosensor is open at 37°C, the M1* mutation creates a *prfA* thermosensor with an open base and, hence, an extensively deregulated PrfA expression at that temperature (Figure S8). This situation made it impossible to study the effect of $SreA_{wt}$ and $SreA_{M1}$ on $prfA_{M1}$-*gfp* expression in vivo (data not shown). We thus analyzed the SreA:$prfA_{M1}$- interaction in vitro (see below).

To investigate further the action of SreA, we examined expression of *prfA-gfp* and SreA transcripts and found it to correlate with the observed protein expression pattern, although the level of these RNA species did not vary as extensively as the protein levels (Figure S9). These results suggest that SreA, by a direct interaction, regulates PrfA expression mainly at the translational level.

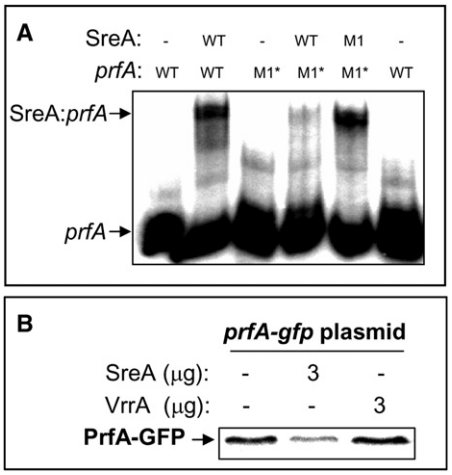

Figure 6. SreA and *prfA* Interact In Vitro

(A) Gel shift experiments with SreA and radioactively labeled *prfA*-UTR. Indicated RNA fragments ($prfA_{wt}$, $prfA_{M1*}$, $SreA_{wt}$, or $SreA_{M1}$) were incubated simultaneously at 37°C for 30 min before separation on native polyacrylamide gels (n = 3). Free *prfA* or *prfA* in complex with SreA is indicated by arrows.

(B) SreA inhibits PrfA-GFP expression in an in vitro transcription/translation assay. The *prfA-gfp* plasmid was incubated in the presence or absence of 3 μg SreA or 3 μg VrrA before samples were taken for western blotting (n = 3).

Could SreB also control PrfA expression in *E. coli*? To answer this question, we expressed SreB together with *prfA-gfp* in *E. coli*. The results indicate that SreB indeed could repress expression of PrfA-GFP in a manner similar to SreA, suggesting that SreB and *prfA* directly interact (Figure 5D).

SreA Is Unable to Interact with the $prfA_{wt}$-UTR at Low Temperatures

We have previously shown that expression of PrfA is low at temperatures below 30°C as the result of an RNA thermosensor within the 5′ UTR (Johansson et al., 2002). To test whether the repressive effect of SreA on PrfA expression was also detected at low temperatures, we grew strains carrying $prfA_{wt}$-*gfp* with either pMK4 or p$sreA_{wt}$ at 30°C or 37°C. As seen in Figure 5E, SreA was not able to repress PrfA expression at 30°C, in contrast to 37°C. This is probably due to an inability of SreA to interact with the closed conformation of the *prfA* thermosensor at 30°C (Johansson et al., 2002). Opening of the thermosensor at 37°C not only allows ribosomal binding, but also permits a possible repressive interaction with SreA.

SreA and the *prfA*-UTR Interact Directly In Vitro

To further validate the SreA:*prfA*-UTR interaction and exclude indirect effects, we synthesized full-length SreA and *prfA*-UTR RNA in vitro, and their putative interaction was studied by native gel shift assay. The addition of $SreA_{wt}$ caused the $prfA_{wt}$-UTR fragment to shift (Figure 6A). Such a shift was almost not detected when $SreA_{wt}$ was added to $prfA_{M1*}$-UTR. In contrast, when $SreA_{M1}$ was added to the $prfA_{M1*}$-UTR fragment, the shift was as strong as that observed for the $SreA_{wt}$:$prfA_{wt}$-interaction. These results show that SreA and *prfA*-UTR directly interact and that the M1:M1* region is essential for such a contact. SAM does not seem to be important for the *trans*-acting function of SreA (Figures 2 and 5B), but it could be hypothesized that SAM affects the SreA:*prfA*-UTR interaction. To test this, we performed native gel shift experiments with $SreA_{wt}$ and the $prfA_{wt}$-UTR fragment in the presence and absence of SAM. Addition of SAM did not affect the interaction between SreA and the *prfA*-UTR, clearly indicating that SAM is not essential for the SreA:*prfA* interaction (Figure S10).

For additional corroboration of the interaction between SreA and *prfA*-UTR, an in vitro transcription/translation approach was undertaken, with $prfA_{wt}$-*gfp* expressed from a plasmid in the presence or absence of SreA RNA. The recently identified ncRNA, VrrA, from *Vibrio cholerae* (Song et al., 2008), was included as a control. Expression of PrfA-GFP was reduced 70%–80% by the addition of SreA, but was unaltered by the addition of VrrA (Figure 6B).

Altogether, our in vivo and in vitro results suggest an ncRNA function for SreA, by which it binds to the 5′ UTR of *prfA* and thereby reduces *prfA* transcript stability and/or *prfA* mRNA translation.

DISCUSSION

In this paper, we describe for the first time, to our knowledge, that a riboswitch known to control transcription of its downstream gene (*cis*-function) also functions as a small noncoding RNA and regulates expression of distally located target mRNAs (*trans*-function). More specifically, we show that the *S*-adenosylmethionine riboswitch SreA binds to the distal side of the *prfA*-untranslated RNA, thereby causing decreased expression of PrfA. Several lines of evidence suggest that the interaction between SreA and the *prfA*-UTR is direct: First, SreA shows a high degree of complementarity between paired region 3 and the distal side of the *prfA*-UTR by in silico analysis (Figure 5A). Second, expression of *prfA-gfp* in the ectopic *E. coli* system is decreased approximately 10 fold in the presence of SreA, compared to the vector control (Figures 5B and C). Third, base-substitution mutations in SreA or in the *prfA*-UTR predicted to destabilize the *prfA*:SreA interaction abolish SreA-mediated repression (Figure 5C; data not shown). Fourth, SreA and the *prfA*-UTR interact directly in vitro requiring the M1:M1* regions, as determined by RNA:RNA gel-shift assay (Figure 6A). Fifth, SreA inhibits synthesis of PrfA-GFP in an in vitro transcription/translation assay (Figure 6B). These two last points exclude effects by other cellular factors (Figures 6A and 6B). Importantly, the interaction between SreA and *prfA* is independent of SAM binding (Figures 2, 5B, and S10). Although SAM is not required for *prfA* and SreA to interact, it does not rule out the possibility that SAM is part of the *prfA*:SreA complex.

Interactions between ncRNAs and specific mRNA targets have previously been reported in various bacterial species, including *L. monocytogenes* (Majdalani et al., 1998; Altuvia et al., 1998; Lenz et al., 2004; Morita et al., 2006; Boisset et al., 2007; Mandin et al., 2007; Sharma et al., 2007; Darfeuille et al., 2007; Urban and Vogel, 2007; Song et al., 2008). On the basis of our findings, we propose that riboswitches can also function as noncoding RNAs. Base-substitutions mutations tested in vivo and in vitro suggest that the SreA:*prfA*-UTR interaction-site resides

approximately 80 bases upstream of the SD site of *prfA* (Figures 5 and 6). This would represent an interaction area unusually distant from the SD site, a situation that has only been reported for a few ncRNAs (Sharma et al., 2007; Darfeuille et al., 2007). In order to understand more precisely the mechanism by which SreA represses *prfA* expression, it will be important to determine exactly the SreA:*prfA*-UTR interaction area, work that is now in progress.

Another SAM riboswitch, SreB, was also able to bind to and control expression of *prfA* and, hence, also *lmo2230* (Figures 1, 3C, 5D, and S11). Interestingly, SreB was not able to control expression of *lmo0049*, suggesting that unique parts of SreA absent in SreB control *lmo0049* expression. We do not know whether other SAM riboswitches can bind to and control expression of *prfA*, although such interactions could be suggested by computer predictions albeit with different strength (Figure S11). In addition, the intracellular stability of the different SAM riboswitches varies dramatically (Table S1).

The absence of SreA increases the amount of PrfA but decreases the amount of *lmo0049*, the latter encoding a quorum-sensing molecule, AgrD, that is important for invasion of intestinal epithelial Caco2-cells (Riedel et al., 2009). Expression of *lmo0049* was not controlled by PrfA (Toledo-Arana et al., 2009). Interestingly, expression of *prfA* was much higher in bacteria exposed to blood, compared to intestinally grown bacteria (Figure S6) (Toledo-Arana et al., 2009). In contrast, *lmo0049* is more expressed in the intestine than in the blood, suggesting that AgrD is more important than PrfA as a regulatory component in the intestine. In agreement with this hypothesis, PrfA has recently been shown to be less critical for expression of virulence genes in the intestine (Toledo-Arana et al., 2009). We do not know the impact of SreA on virulence, but its opposite function for expression of two important virulence activators (AgrD and PrfA) suggest it to be central. We have measured the absolute number of SreA in the bacterium. Our results suggest that only seven copies of SreA/bacterium are present when the bacteria are grown in BHI medium to an OD_{600} of 0.4 (Table S1). SreA is more abundant during *L. monocytogenes* exposure to blood and intestinal infection, compared with growth in BHI medium, with its total number increasing to 20–40 molecules/bacterium (Table S1; Figure S11) (Toledo-Arana et al., 2009). *prfA* and SreA are equally abundant when bacteria are exposed to blood (Figure S6). In contrast, the amount of *prfA* is much lower during growth in the intestine (less than one copy/bacteria). Clearly, the physiological roles of SreA and SreB remain to be precised, but our work suggest a role for them (as well as other listerial SAM-I riboswitches) to down-regulate PrfA-expression in compartments (i.e., intestine) where other regulatory pathways are active (i.e., AgrD).

PrfA expression is controlled at several levels: transcriptional, translational, and posttranslational (Scortti et al., 2007). As we have previously shown, expression of PrfA is inhibited during growth at low temperatures because of an RNA thermosensor within the 5′ UTR (Johansson et al., 2002). Interestingly, SreA is not able to interact with the thermosensor at low temperatures when the latter is present in the most stable conformation (Figure 5E) (Johansson et al., 2002). This implies a function of SreA on PrfA expression only at temperatures permissive for infection (i.e., 37°C) and not at lower temperatures. Another layer of complexity is that SreA expression is PrfA dependent, thereby forming a regulatory loop where a high level of PrfA activates transcription of SreA, which, in turn, down-regulates PrfA expression (Figures 3 and 4).

Finally, our data do not rule out a regulatory role for the SAM riboswitches when they are part of a longer, antiterminated, transcript. We anticipate that other classes of riboswitch elements, controlling their downstream genes by a transcription termination mechanism, might also be able to function as ncRNAs in a manner similar to SreA.

EXPERIMENTAL PROCEDURES

Oligonucleotides, Strains, Plasmids, Growth Media, and Culture Conditions

The oligonucleotides used in this study are listed in Table S3. The strains and plasmids used in this study are listed in Table S4. *L. monocytogenes* strains were grown in BHI broth or agar (Fluka), and *E. coli* Novablue (Novagen) was grown in Luria-Bertani (LB) broth and agar. For RNA isolation, *L. monocytogenes* overnight cultures were diluted 100-fold and grown to the indicated optical density (0.4) in the absence of antibiotics. For knockout constructions and overnight cultures, antibiotics were added at the following concentrations: carbenicillin, 100 $\mu g/ml^{-1}$; chloramphenicol, 7 $\mu g/ml^{-1}$; and erythromycin, 7 $\mu g/ml^{-1}$. All strains were grown at 37°C with aeration. The human-derived epithelial cell line HeLa was cultured in RPMI 1640 medium supplemented with 10% FBS and 5 mM glutamine. The cell line was maintained at 37°C in a 5% CO_2-air atmosphere.

Site-Directed Mutagenesis

In order to obtain site-specific mutations in SreA, we used the Quikchange site-directed mutagenesis kit from Stratagene. Plasmid pMK4 harboring the *sreA* fragment was used as template in the mutagenesis reactions. To achieve a SreA construct unable to bind SAM, oligonucleotides #47basesub1-U and #47basesub1-L were used (Table S3). The resulting construct was sequenced, and the correct plasmid was used as template together with the oligonucleotides #47basesub2-U and #47basesub2-L (Table S3) to create a SreA construct unable to form an antitermination structure. The resulting plasmid ($psreA_{NSB}$) was sequenced, to ensure that no other changes had occurred. To achieve a SreA construct lacking the putative M1 site ($SreA_{M1}$), oligonucleotides SreAM1-U and SreAM1-U were used (Table S3). The resulting construct was sequenced. $SreA_{M1}$ could not be created unless the −10 region preceding SreA was mutated from TAATAT to TAGTAT, thereby lowering the total amount of SreA (data not shown). This base-pair replacement was also introduced into the $SreA_{wt}$ construct. The $prfA_{M1}$-GFP was made as follows: Plasmid pEGFP-*prfA* (Johansson et al., 2002) was used as a template with the oligonucleotides PrfAM1*-U and PrfAM1*-L (Table S3). The resulting plasmid was sequenced, to ensure that no other changes had occurred.

Statistical Analysis

Statistical analysis was performed by using Student t test (two-tailed distribution, two-sample equal variance) when indicated in the figure legends.

RNA Isolation

Total cellular RNA was isolated from *L. monocytogenes* by dissolving pelleted cultures (20 ml, A_{600} = 0.4) in resuspension solution (10% glucose, 12.5 mM Tris [pH 7.6], and 5 mM EDTA) and fresh EDTA (0.5 M). Samples were immediately transferred to bead beater tubes with roughly 0.4 g glass beads and 500 µl of acid phenol (pH 4.5). The bacteria were disrupted using a mini bead beater (Biospec products) for 75 s. After centrifugation (5 min, 20 800 × g) RNA was recovered by addition of 1 ml of trizol and 100 µl of chloroform/isoamylalcohol (24:1), followed by centrifugation. Samples were thereafter subjected to two additional chloroform/IAA extractions. The aqueous phase was precipitated by adding isopropanol (0.7×) and incubated at

−20°C for 20 min. For collection of the pellet, the RNA samples were centrifuged for 25 min. The pellet was dissolved in 200 μl of RNase-free water.

For removal of the remaining DNA, samples were treated with 20 U of DNaseI (Ambion) for 45 min at 37°C. The reaction was terminated by addition of phenol/chloroform/IAA (1:24:1 [pH 6.6]). Centrifuged samples were chloroform/IAA extracted and ethanol precipitated. The pellet was resuspended in 200 μl RNase-free water, RNA concentration was measured on a Nanodrop (Nanodrop ND-1000 Spectrophotometer), and the RNA integrity was determined on a 1.2% agarose gel. Only RNA samples showing distinct nonprocessed precursors to ribosomal RNA were used in the following experiments.

Northern Blot

For northern blotting, 20 μg of total RNA was separated on a formaldehyde agarose gel prior to blotting as described (Toledo-Arana et al., 2009). The Hybond-N membrane was subsequently hybridized with ^{32}P α-labeled DNA fragments amplified with corresponding primers. Northern blots were developed, and band intensities were measured in the STORM machine (Molecular Dynamics). Primers used are listed in Table S3. To amplify a DNA fragment for detection of *lmo2230*, *lmo0049*, SreA, SreB *prfA*, *gfp*, *hly*, *lmo2419*, and tmRNA, we used primers lmo2230-U and lmo2230-L, lmo0049-U and lmo0049-L, sreA-U and sreA-L, sreB-U and sreB-L, prfA-U and prfA-L, prfA-U and gfp-L, hly-U and hly-D, lmo2419-U and lmo2419-L, and tmRNA-U and tmRNA-L, respectively.

RNA Stability

Indicated *L. monocytogenes* strains were grown at 37°C in a shaking water bath, until A_{600} = 0.4. Initiation of transcription was stopped by the addition of rifampicin to 250 μg/ml, and samples were collected at indicated time points for RNA isolation and qRT-PCR.

Real-Time Quantitative PCR with Reverse Transcriptase

Real-time PCR quantification of RNA templates was conducted with a Biorad iCyclerIQ according to the manufacturer's description. In brief, an iScript one-step RT-PCR kit with SYBR GREEN (BioRad) was used with 5 ng (*lmo2230*, *lmo0049*, SreA, SreB, SreC, SreD, SreE, SreF, SreG, and *prfA*) or 250 pg (tmRNA) total RNA template in a total volume of 25 μl. Primers used are listed in Table S3. Cycles were as follows: 50°C for 10 min, 95°C for 5 min, (95°C for 10 s and 55°C for 30 s) 45 times. qRT-PCR data in Figures 1 and 2 were compared to Δ*sreA* plus pMK4 using Student t test (two-tailed; *** $p < 0.001$, * $p < 0.05$).

Determination of SreA Molecules/Bacterium

qRT-PCR was performed with different dilutions of purified SreA transcript used as a standard curve and total RNA from cultures isolated at OD_{600} = 0.4. By this, the total mass of SreA/ml culture could be determined. By knowing the number of bacteria/ml culture, the molecular mass of SreA and the Avogadro constant, the number of SreA/bacterium could be measured (7 ± 3).

SDS-PAGE and Western Blotting

The different cultures were grown in BHI (*L. monocytogenes*) or LB medium (*E. coli*) to an optical density of OD_{600} = 0.4. Bacteria were centrifuged and resuspended in buffer A (200 mM KCl, 50 mM Tris-HCl [pH = 8.0], 1 mM EDTA, and 10% glycerol). The suspension was disrupted using a bead-beater for 1.5 min at maximum speed. After 2 min on ice, the suspension was centrifuged at 15,000 rpm for 5 min, and the supernatant (cytoplasmic fraction) was removed. Protein samples were separated on a 12% polyacrylamide gel electrophoresis before being transferred onto a PVDF membrane using a semidry blotting apparatus. Development of the membrane essentially followed the protocol of the ECL$^+$ western blotting kit (Amersham), using anti-PrfA (IS3b - R78), anti-σ^B, anti-GFP (BD-living colors), or anti-GroEL as primary antibodies and HRP-conjugated anti-rabbit or anti-goat as secondary antibodies (Bio-Rad). Measurement of protein expression was carried out in the STORM machine (Molecular Dynamics).

In Vitro Transcription Termination Experiments

PCR was used to generate DNA templates containing either T7 promoter or native promoter in front of the SreA riboswitch element using primers 47-R or sreApT7U together with lmo2419-L (Table S3). One microgram of PCR product was used as template. Reactions were performed in a volume of 30 μl and contained for the T7 polymerase reactions 0.2 mM ATP, GTP, CTP, 5 μCi α-32 P UTP, and 50 U T7 RNA polymerase, and for the RNA holoenzyme reactions 0.25 mM ATP, GTP, CTP, 5 μCi α-32 P UTP, and 2.5 U *E. coli* RNA Polymerase Holoenzyme (Epicenter Biotechnologies). Both T7 polymerase and RNA holoenzyme reactions were incubated in the presence of 40 mM Tris-HCl, 6 mM $MgCl_2$, 2 mM spermidine, 10 mM dithiothreitol (pH 7.9 at 25°C), and 40 U Ribolock TM RNase inhibitor (Fermentas) for 2 hr at 37°C. SAM was added at a concentration of 50 μM. Reactions were denatured in the presence of formamide dye mix and were separated by 8% urea-PAGE. Gels were dried and visualized by PhosphorImager.

RNA-RNA Gel Shift

RNA gel shift assays were performed as described earlier (Mandin et al., 2007). In brief, uniformly ^{32}P-UTP-labeled $prfA_{wt}$ and $prfA_{M1}$. were synthesized in vitro using T7 RNA polymerase and PCR fragments as template, before purification of the RNA fragments on Urea-PAGE gel. The PCR fragments were amplified with prfA-pT7 and prfA-5 oligonucleotides and p$prfA_{wt}$-*gfp* or p$prfA_{M1}$.-*gfp* as template (Table S3). "Cold" $SreA_{wt}$ and $SreA_{M1}$ were synthesized in vitro using T7 RNA polymerase and PCR fragments as template. The PCR fragments were amplified with SreA-pT7U and SreA-T7U oligonucleotides and p$sreA_{wt}$ and p$sreA_{M1}$ as template (Table S3). Complex formation assays were performed at 37°C for 30 min in a buffer containing 20 mM Tris-HCl (pH 7.5), 10 mM $MgCl_2$, and 150 mM NaCl in the presence of 600 nM of each RNA-fragment. When indicated, 50 μM of SAM was added to the reactions 15 min after complex formation initiation incubation.

In Vitro Transcription/Translation

Three micrograms of in vitro transcribed $SreA_{wt}$ or VrrA (PCR synthesized using oligos T7 and VrrA-D) was incubated together with 0.3 μg of pT7p$prfA_{wt}$-*gfp* plasmid (T7 driven *prfA-gfp*, amplified using primers prfA-pT7 and gfpD with p$prfA_{wt}$-*gfp* as template and inserted into pGEM-T) in an S30 T7 high yield in vitro Transcription/Translation Kit (Promega) according to the manufacturer's instructions. In brief, the mixtures were incubated at 25°C for 5 min before transfer to 37°C for an additional 5 min. Samples were acetone-precipitated, resuspended in sample buffer, and separated on a 12% polyacrylamide gel electrophoresis, before being transferred onto a PVDF membrane using a wet blotting apparatus (Biorad). Development of the membrane essentially followed the protocol of the ECL$^+$ western blotting kit (Amersham), using anti-GFP (BD-living colors) as primary antibodies and HRP-conjugated anti-goat as secondary antibodies (Bio-Rad).

Fluorescent Imaging on Agar Plate

Bacterial strains were streaked onto a LB-plate containing carbenicillin (100 μg/ml) and kanamycin (50 μg/ml) and were grown overnight. Fluorescence imaging was performed with an IVIS Spectrum imaging system (Xenogen). A GFP filter (excitation wavelength 445–490 nm and emission 515–575 nm) was used for acquiring fluorescence imaging. Identical illumination settings, such as exposure time (1 s) and field of views (15 × 15 cm), were used for acquiring all images. Fluorescence emission was normalized to photons per second per centimeter squared per steradian (p s-1 cm-2 sr-1). Images were acquired and analyzed using Living Image 3.0 software (Xenogen).

cDNA Labeling and Hybridization

Chromosomal DNA (30 ng) isolated from *L. monocytogenes* strains EGDe or Δ*sreA* was ^{33}P-labeled using a random primed DNA labeling kit (Boehringer Manheim). Labeled genomic DNAs were purified prior to hybridization using QIAquick columns (QIAGEN). For cDNA synthesis, random hexamers primers were used in reverse transcription reactions in the presence of [α-^{33}P]dCTP (2000–3000 Ci mmol^{-1}, Amersham). One microgram of total RNA and 50 U AMV reverse transcriptase (Roche) with Rnase H activity were used. Labeled cDNA was purified prior to hybridization using a QIAquick column (QIAGEN).

Hybridization and washing steps were carried out using SSPE buffer (0.18 M NaCl, 10 mM NaH_2PO_4, and 1 mM EDTA [pH 7.7]). Macroarrays were pre-wet in 2× SSC and prehybridized for at least 2 hr in hybridization solution

(5× SSPE, 2% SDS, 1× Denhardt's reagent, and 100 μg of sheared salmon sperm DNA/ml^{-1}) at 65°C in roller bottles. Hybridization was carried out for 20 hr at 65°C in hybridization solution and the entire spin-purified cDNA probe. For each strain, two independent RNA preparations were tested, and two cDNAs from each of the RNA preparations were hybridized to two sets of arrays and analyzed.

Membranes were scanned using a 445SI phosphorImager (Molecular Dynamics). The ArrayVision software (Imaging Research, St Catherines, ON, Canada) was used for quantification of the hybridization intensities and for normalization. For identification of genes with statistically significant changes in expression SAM (Significance Analysis of Microarrays, http://www-stat.stanford.edu/~tibs/SAM/) was used. Genes whose expression change was 2-fold in all arrays and significant according to this analysis were taken into account (Table S2). All gene-array data have been deposited at ArrayExpress with the accession number E-MTAB-118.

Cell Culture, Infection, and Isolation of RNA

Wild-type *L. monocytogenes* was grown in 100 mm diameter tissue culture plates with and without HeLa cells. For extracellular experiments, *Listeria* was allowed to grow for 4 hr in supplemented RPMI 1640 medium. For intracellular experiments, *Listeria* was allowed to infect the cells. After 1 hr of infection, the plate containing HeLa cells and *L. monocytogenes* was washed with fresh supplemented RPMI 1640 medium twice, and a final concentration of 100 μg/ml^{-1} of gentamicin was added to the fresh medium. *L. monocytogenes* was allowed to grow in the cells for 4 hr before bacteria and cells were harvested from the plate and centrifuged at 13,000 rpm. Total RNAs were extracted by use of the Fast RNA Pro Blue kit (Q-Biogen, MP Biomedicals, Illkirch, France), following the manufacturer's instructions. For qRT-PCR, total RNAs were treated with 20 U of DNase I (Ambion) for 1 hr at 37°C, and concentrations were determined with Nanodrop (Nanodrop ND-1000 Spectrophotometer).

Complementation

For construction of *sreA* and *sreB* complemented strains, the corresponding DNA fragment was amplified with PCR (oligonucleotides; *sreA*:#47 F and R and *sreB*: #50 F and R) (Table S3) and was ligated at 16°C overnight into pGEM-T easy vector (Promega) system with T4 DNA ligase (Usb). JM109 high efficient competent cells (Promega) were transformed with pGEM-*sreA* or pGEM-*sreB*, and the plasmid was thereafter recovered from overnight cultured cells with QIAprep spin miniprep (QIAGEN). The pGEM construct were digested with EcoRI (Roche) and SalI (Roche), and the fragment was purified with a gel extraction kit (QIAGEN) and was ligated with EcoRI and SalI digested pMK4 (19). JM109 cells were transformed with the pMK4 constructs, and transformants were spread on LB plates with carbenicillin (50 μg/ml). Plasmids were harvested as previously and were transformed into *L. monocytogenes ΔsreA* cells by electroporation (2.4 kV, 200 Ω, 25 μF) and were spread on chloramphenicol plates (7 μg/ml). Sequence was verified by using Dyenamic ET terminator kit.

ACCESSION NUMBERS

All gene-array data have been deposited at ArrayExpress with the accession number E-MTAB-118.

SUPPLEMENTAL DATA

Supplemental Data include Supplemental Experimental Procedures, 11 figures, and four tables and can be found with this article online at http://www.cell.com/supplemental/S0092-8674(09)01186-6.

ACKNOWLEDGMENTS

We thank S. Gottesman, T. Geissmann, and B. Guo, for critical reading of the manuscript. We thank A. Toledo-Arana and M. Vergassola for computer predictions, Christophe Rusniok for data submission, N. Sesto and T. Geissmann for technical assistance, and S. Engelmann for SigB antibody. J.J. is supported by the Wenner-Gren Foundations, Umeå University, the Swedish Research Council (grants 2008-58X-15144-05-3 and 621-2006-4450), and EU (BacRNA 2005 contract number 018618). Work in the laboratory of P.C. received financial support from Institut Pasteur (GPH 9), INSERM, INRA, EU (BacRNA 2005 contract number 018618), ERC, and ANR (ANR-05-MIIM-026-01). P.C. is an international research scholar from the Howard Hughes Medical Institute.

Received: April 3, 2009
Revised: July 16, 2009
Accepted: August 26, 2009
Published: November 12, 2009

REFERENCES

Altuvia, S., Zhang, A., Argaman, L., Tiwari, A., and Storz, G. (1998). The *Escherichia coli* OxyS regulatory RNA represses *fhlA* translation by blocking ribosome binding. EMBO J. *17*, 6069–6075.

Boisset, S., Geissmann, T., Huntzinger, E., Fechter, P., Bendridi, N., Possedko, M., Chevalier, C., Helfer, A.C., Benito, Y., Jacquier, A., et al. (2007). *Staphylococcus aureus* RNAIII coordinately represses the synthesis of virulence factors and the transcription regulator Rot by an antisense mechanism. Genes Dev. *21*, 1353–1366.

Darfeuille, F., Unoson, C., Vogel, J., and Wagner, E.G. (2007). An antisense RNA inhibits translation by competing with standby ribosomes. Mol. Cell *26*, 381–392.

Griffiths-Jones, S., Moxon, S., Marshall, M., Khanna, A., Eddy, S.R., and Bateman, A. (2005). Rfam: annotating non-coding RNAs in complete genomes. Nucleic Acids Res. *33*, D121–D124.

Guillier, M., Gottesman, S., and Storz, G. (2006). Modulating the outer membrane with small RNAs. Genes Dev. *20*, 2338–2348.

Henkin, T.M. (2008). Riboswitch RNAs: using RNA to sense cellular metabolism. Genes Dev. *22*, 3383–3390.

Johansson, J., and Cossart, P. (2003). RNA-mediated control of virulence gene expression in bacterial pathogens. Trends Microbiol. *11*, 280–285.

Johansson, J., Mandin, P., Renzoni, A., Chiaruttini, C., Springer, M., and Cossart, P. (2002). An RNA thermosensor controls expression of virulence genes in *Listeria monocytogenes*. Cell *110*, 551–561.

Lenz, D.H., Mok, K.C., Lilley, B.N., Kulkarni, R.V., Wingreen, N.S., and Bassler, B.L. (2004). The small RNA chaperone Hfq and multiple small RNAs control quorum sensing in *Vibrio harveyi* and *Vibrio cholerae*. Cell *118*, 69–82.

Lu, C., Smith, A.M., Fuchs, R.T., Ding, F., Rajashankar, K., Henkin, T.M., and Ke, A. (2008). Crystal structures of the SAM-III/SMK riboswitch reveal the SAM-dependent translation inhibition mechanism. Nat. Struct. Mol. Biol. *15*, 1076–1083.

Majdalani, N., Cunning, C., Sledjeski, D., Elliott, T., and Gottesman, S. (1998). DsrA RNA regulates translation of RpoS message by an anti-antisense mechanism, independent of its action as an antisilencer of transcription. Proc. Natl. Acad. Sci. USA *95*, 12462–12467.

Mandin, P., Repoila, F., Vergassola, M., Geissmann, T., and Cossart, P. (2007). Identification of new noncoding RNAs in *Listeria monocytogenes* and prediction of mRNA targets. Nucleic Acids Res. *35*, 962–974.

McDaniel, B.A., Grundy, F.J., Artsimovitch, I., and Henkin, T.M. (2003). Transcription termination control of the S box system: direct measurement of S-adenosylmethionine by the leader RNA. Proc. Natl. Acad. Sci. USA *100*, 3083–3088.

Milohanic, E., Glaser, P., Coppée, J.Y., Frangeul, L., Vega, Y., Vázquez-Boland, J.A., Kunst, F., Cossart, P., and Buchrieser, C. (2003). Transcriptome analysis of *Listeria monocytogenes* identifies three groups of genes differently regulated by PrfA. Mol. Microbiol. *47*, 1613–1625.

Moors, M.A., Levitt, B., Youngman, P., and Portnoy, D.A. (1999). Expression of listeriolysin O and ActA by intracellular and extracellular *Listeria monocytogenes*. Infect. Immun. *67*, 131–139.

Montange, R.K., and Batey, R.T. (2006). Structure of the S-adenosylmethionine riboswitch regulatory mRNA element. Nature *441*, 1172–1175.

Morita, T., Mochizuki, Y., and Aiba, H. (2006). Translational repression is sufficient for gene silencing by bacterial small noncoding RNAs in the absence of mRNA destruction. Proc. Natl. Acad. Sci. USA *103*, 4858–4863.

Nudler, E. (2006). Flipping riboswitches. Cell *126*, 19–22.

Rehmsmeier, M., Steffen, P., Höchsmann, M., and Giegerich, R. (2004). Fast and effective prediction of microRNA/target duplexes. RNA *10*, 1507–1517.

Renzoni, A., Dramsi, S., and Cossart, P. (1999). PrfA, the transcriptional activator of virulence genes, is upregulated during interaction of *Listeria monocytogenes* with mammalian cells and in eukaryotic cell extracts. Mol. Microbiol. *34*, 552–561.

Riedel, C.U., Monk, I.R., Casey, P.G., Waidmann, M.S., Gahan, C.G., and Hill, C. (2009). AgrD-dependent quorum sensing affects biofilm formation, invasion, virulence and global gene expression profiles in *Listeria monocytogenes*. Mol. Microbiol. *71*, 1177–1189.

Romby, P., Vandenesch, F., and Wagner, E.G.H. (2006). The role of RNAs in the regulation of virulence-gene expression. Curr. Opin. Microbiol. *9*, 229–236.

Roth, A., and Breaker, R.R. (2009). The structural and functional diversity of metabolite-binding riboswitches. Annu. Rev. Biochem. *78*, 305–334.

Scortti, M., Monzó, H.J., Lacharme-Lora, L., Lewis, D.A., and Vázquez-Boland, J.A. (2007). The PrfA virulence regulon. Microbes Infect. *9*, 1196–1207.

Sharma, C.M., Darfeuille, F., Plantinga, T.H., and Vogel, J. (2007). A small RNA regulates multiple ABC transporter mRNAs by targeting C/A-rich elements inside and upstream of ribosome-binding sites. Genes Dev. *21*, 2804–2817.

Song, T., Mika, F., Lindmark, B., Liu, Z., Schild, S., Bishop, A., Zhu, J., Camilli, A., Johansson, J., Vogel, J., et al. (2008). A new *Vibrio cholerae* sRNA modulates colonization and affects release of outer membrane vesicles. Mol. Microbiol. *70*, 100–111.

Toledo-Arana, A., Repoila, F., and Cossart, P. (2007). Small noncoding RNAs controlling pathogenesis. Curr. Opin. Microbiol. *10*, 182–188.

Toledo-Arana, A., Dussurget, O., Nikitas, G., Sesto, N., Guet-Revillet, H., Balestrino, D., Loh, E., Gripenland, J., Tiensuu, T., Vaitkevicius, K., et al. (2009). The transcriptional landscape of *Listeria monocytogenes*: switch from saprophytism to virulence. Nature *459*, 950–956.

Urban, J.H., and Vogel, J. (2007). Translational control and target recognition by *Escherichia coli* small RNAs *in vivo*. Nucleic Acids Res. *35*, 1018–1037.

Vogel, J., and Wagner, E.G.H. (2007). Target identification of small noncoding RNAs in bacteria. Curr. Opin. Microbiol. *10*, 262–270.

Winkler, W.C., Nahvi, A., Sudarsan, N., Barrick, J.E., and Breaker, R.R. (2003). An mRNA structure that controls gene expression by binding S-adenosylmethionine. Nat. Struct. Biol. *10*, 701–707.

Whitford, P.C., Schug, A., Saunders, J., Hennelly, S.P., Onuchic, J.N., and Sanbonmatsu, K.Y. (2009). Nonlocal helix formation is key to understanding S-adenosylmethionine-1 riboswitch function. Biophys. J. *96*, L7–L9.